MISSOURI S&T

Missouri University of Science and Technology

Scholars' Mine

Materials Science and Engineering Faculty Research & Creative Works

Materials Science and Engineering

Growth and Magnetic Properties of MnO₂-δ Nanowire Microspheres

Jinbo Yang

X.-D. Zhou
Missouri University of Science and Technology

Satish K. Malik

C. S. Wang

et. al. For a complete list of authors, see https://scholarsmine.mst.edu/matsci_eng_facwork/1438

Follow this and additional works at: https://scholarsmine.mst.edu/matsci_eng_facwork

Part of the Chemistry Commons

Recommended Citation

J. Yang et al., "Growth and Magnetic Properties of MnO₂-δ Nanowire Microspheres," *Applied Physics Letters*, American Institute of Physics (AIP), Oct 2004.
The definitive version is available at https://doi.org/10.1063/1.1805699

Growth and magnetic properties of MnO$_{2-\delta}$ nanowire microspheres

J. B. Yang,[a)] X. D. Zhou, and W. J. James
Graduate Center for Materials Research and Departments of Physics and Chemistry,
University of Missouri–Rolla, Rolla, Missouri 65409

S. K. Malik
Tata Institute of Fundamental Research, Colaba, Mumbai 400-005, India

C. S. Wang
School of Physics, Peking University, Beijing 100871, People's Republic of China

We report the synthesis of MnO$_{2-\delta}$ microspheres using hydrothermal and conventional chemical reaction methods. The microspheres of MnO$_{2-\delta}$ consist of nanowires having a diameter of 20–50 nm and a length of 2–8 μm. The value of oxygen vacancy δ estimated from x-ray photoelectron spectrum is 0.3. The magnetization versus temperature curve indicates a magnetic transition at about 13 K. It is found that a parasitic ferromagnetic component is imposed on the antiferromagnetic structure of MnO$_{2-\delta}$, which might result from distortion of the lattice structure due to oxygen vacancies. The magnetic transition temperature T_N is about 10 K lower than that of the bulk MnO$_2$ single crystal. © *2004 American Institute of Physics.* [DOI: 10.1063/1.1805699]

The possibility of controlling the structure and the chemical composition of materials at the nanoscale level is of great interest for both basic science and technological applications. In particular, one dimensional (1D) nanometric structures of oxides have attracted intensive attention.[1–4] For example MnO$_2$ has distinctive properties which have enabled its use as catalysts, ion-sieves, and electrode materials.[5–7] Both α- and γ- MnO$_2$ are potential candidates for cathode and catalysts in Li/MnO$_2$ batteries.[5] They can be converted into Li$_{1-x}$Mn$_2$O$_4$ cathode by electrochemical Li$^+$ intercalation, in which Li$^+$ was inserted or extracted during the charging or discharge process. MnO$_2$ nanowires are of great interest due to the fact that their morphology simultaneously minimize the distance over which Li$^+$ must diffuse during the discharge and charging processes.[8] This may provide the opportunity to determine the theoretical operating limits of a lithium battery as the 1D nanowire is the smallest structure for the efficient electron transport. MnO$_2$ nanowires or nanostructure materials also contain much higher surface area which may become more ideal host materials for the insertion and extraction of lithium ions and chemical reactions. Therefore, well-defined 1D nanostructures appear as a much better candidate for studies on the space-confined transport phenomena as well as applications. Considerable effort has been made to prepare bulky or nanocrystalline MnO$_2$ with different structures.[9–12] Recently, single-crystal MnO$_2$ nanowires have been synthesized using a hydrothermal method.[13] MnO$_2$ also possesses an interesting magnetic structure.[14–17] Very few investigations on the magnetic properties of nano-sized Mn-oxides have been reported. In this letter, we report the synthesis of microspheres of MnO$_{2-\delta}$ consisting of nanowires. The microspheres were prepared using both hydrothermal and room temperature chemical reaction methods. The structure, morphology, composition, and magnetic properties of the Mn-oxide microspheres were studied using x-ray diffraction (XRD), scanning electron microscopy (SEM), transmission electron microscopy (TEM),

magnetic measurements and x-ray photoelectron spectroscopy (XPS).

The materials synthesized here were prepared by oxidation of hydrated manganese sulfate MnSO$_4$.H$_2$O with an equal amount of ammonium persulfate (NH$_4$)$_2$S$_2$O$_8$.[13] MnSO$_4$.H$_2$O (0.08 mol) and (NH$_4$)$_2$S$_2$O$_8$ (0.08 mol) were dissolved in 150 ml distilled water at room temperature to form a clear solution. Half of the solution was transferred into a stainless steel autoclave, sealed and maintained at 120°C for 12 h. Another half of the solution was kept at room temperature in air for 6 h. After the reaction, the resulting black solid from each solution was filtered and washed with distilled water and acetone several times, then dried at 60°C for 24 h. XRD using Cu K_α radiation shows the material to be single phase, α-MnO$_2$. The magnetization curves of the samples were measured using a superconducting quantum interference device magnetometer in a field of up to 6 T from 1.5 to 300 K. The morphology was studied using SEM(JEOL-6340F) and TEM. X-ray photoelectron spectra were collected using a "KRATOS" model AXIS 165 XPS spectrometer with a Mg source and an Al monochrometer.

Figure 1 shows the x-ray diffraction patterns of the samples obtained by both methods. The diffraction peaks can be indexed to α-MnO$_2$ with lattice parameters a=9.784 Å and c=2.863 Å, space group $I4/m$. The XRD pattern of the
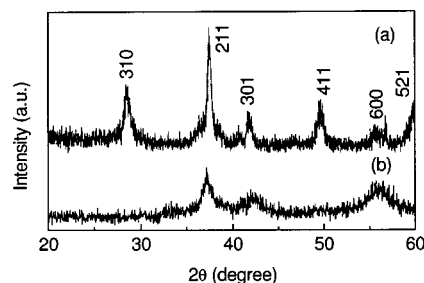

FIG. 1. X-ray diffraction patterns of the sample prepared by the hydrothermal method (a) and room temperature reaction (b).
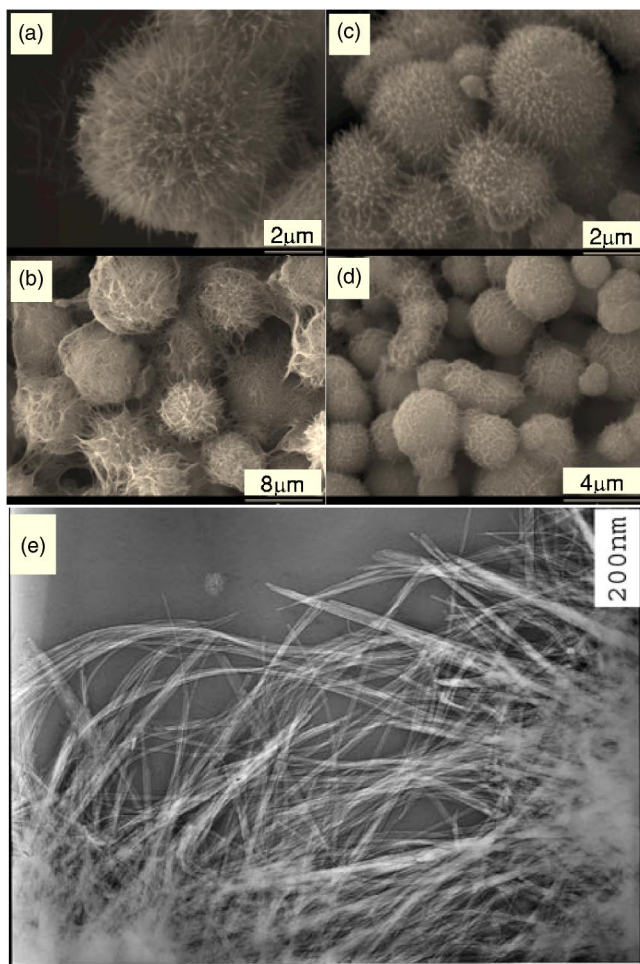
a)Electronic mail: jinbo@umr.edu

FIG. 2. The SEM (a)–(d) and TEM(e) images of the Mn-oxides: (a) and (b) prepared by hydrothermal method; (c) and (d) prepared at room temperature; (e) TEM image prepared by hydrothermal method.

FIG. 3. Room temperature x-ray photoelectron spectrum of $MnO_{2-\delta}$ prepared by the hydrothermal method.

spheres by aggregation of the nanowires is favored by a decrease in the total surface energy of the system.

A typical room temperature x-ray photoelectron spectrum of the $Mn_{2-\delta}$ prepared by the hydrothermal method is plotted in Fig. 3. The peaks of Mn $(3s, 3p, 2p, 2s)$ and O $(1s, 2s)$ are observed. Auger peaks from Mn and O are also observed as O *KLL* and Mn *LMM* lines. The binding energies of the Mn $2p3/2$ and $2p1/2$ states are 641.5 and 653.6 eV, respectively, which are lower than those of the standard MnO_2 (642.1 and 653.8 eV).[18] The decrease in binding energy is likely due to the oxygen vacancies formed in these materials which would decrease the Mn–O bond strength. The estimated relative ratio of Mn to O is 37:63 corresponding to a composition of about $MnO_{1.7}$.

Figure 4 shows the zero field cooling (ZFC) and field cooling (FC) magnetization curves of $Mn_{2-\delta}$ prepared by the hydrothermal method measured under different magnetic fields. A kink is observed at about 13 K in Figs. 4(a) and

room temperature treated sample [Fig. 1(b)] shows much broader, and less intensive peaks, due to its smaller grain size and the many crystal defects. There are some changes in the relative peak intensities in Fig. 1(b), suggesting a preferred orientation among the Mn-oxide grains. The mean size of the particles [Fig. 1(a)] is about 40 nm as determined by the Scherrer formula using the width of the [211] peak from Fig. 1(a), and was further confirmed by SEM and TEM imaging (Fig. 2).

Figure 2 shows the SEM [(a)–(d)] and TEM(e) images of the samples prepared by the two methods. Figures 2(a) and 2(b) show a sea urchin-like sphere with a diameter of $4-8$ μm for the sample prepared by the hydrothermal method. These microspheres consist of bundles of small wires with a diameter of $20-50$ nm [see TEM image (e)]. Figures 2(c) and 2(d) show the typical morphology of the MnO_2 obtained by the reaction carried out at room temperature. The diameter of these microspheres varies from 1 to 4 μm. The microspheres are also made up to smaller needle-like wires, however, they are not sharply defined as compared to the samples made by the hydrothermal method. The hydrothermal treatment increases the diameter of the microspheres and the length of the nanowires. It is found that the concentration of the solution is very important in forming the microspheres. The microspheres can be synthesized when the Mn^{2+} concentration is higher than 0.3 mol/L. It suggests that, at high Mn^{2+} concentrations, the formation of micro-
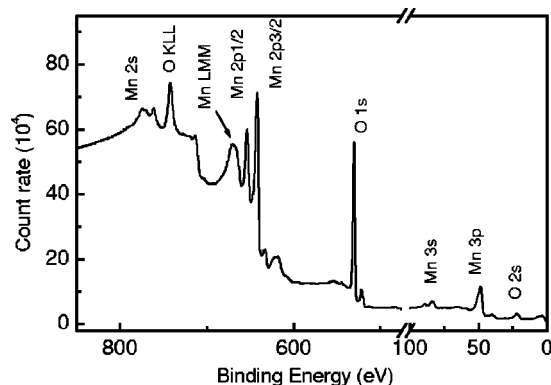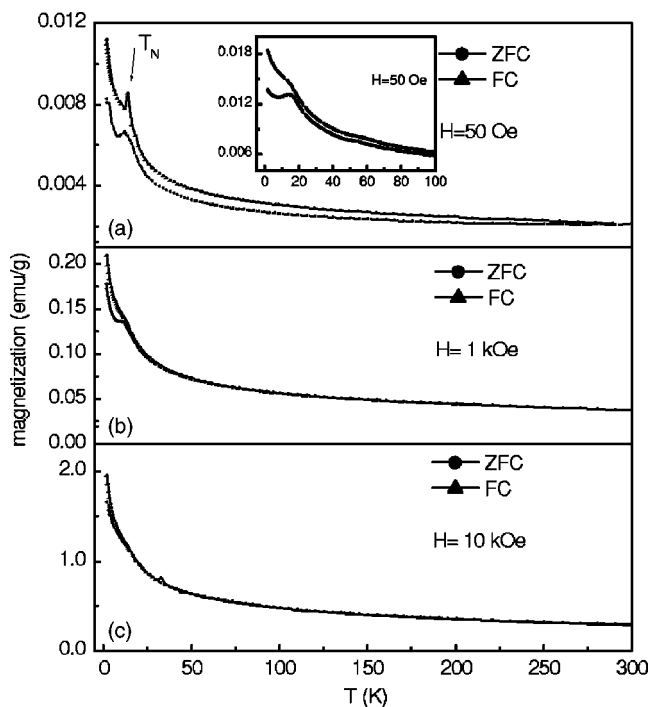

FIG. 4. The temperature dependence of the magnetization curves under zero field cooling (ZFC) and field cooling (FC) for $MnO_{2-\delta}$ prepared by the hydrothermal method: (a) $H=50$ Oe, (b) $H=1$ kOe (c) $H=10$ kOe. The inset in (a) is for the sample made at room temperature.
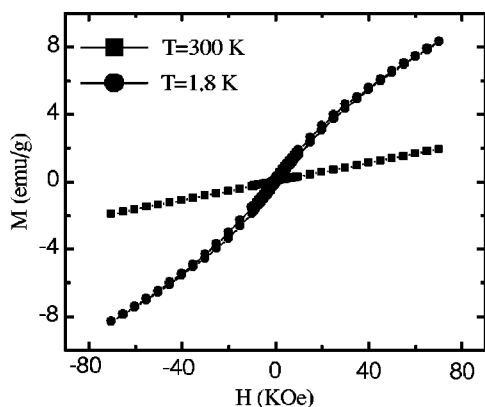
FIG. 5. The magnetization vs applied magnetic field curves of $MnO_{2-\delta}$ prepared by the hydrothermal method at different temperatures.

4(b), corresponding to the Néel magnetic transition temperature T_N. This temperature is lower than that of a MnO_2 single crystal[17] $T_N = 24.5$ K, which is due to the small grain size effect.[19] The kink as well as the difference between the ZFC and FC curves becomes smaller as the applied magnetic field increases. The inset in Fig. 4(a) shows the ZFC and FC curves of the sample prepared at room temperature. A similar phenomenon is observed, except that the transition peaks are much broader and the magnetization value is higher, which may be due to more defects and a larger distortion in this sample. Figure 5 is the magnetization versus applied magnetic field curves of the sample prepared by the hydrothermal method. At 1.8 K, the $M-H$ curve shows a small hysteresis, which indicates that a ferromagnetic component is superposed on the antiferromagnetic curve. This agrees with the $M-T$ curves in that the magnetization increases with decreasing temperature suggesting a ferrimagnetic or ferromagnetic structure is formed in this compound. At 300 K, nearly linear $M-H$ curves reveal that a paramagnetic state exists in this temperature range. The ferromagnetic component at low temperature may result from the noncollinear molecular field that cants the two antiparallel sublattices due to the distortion of the crystal structure, especially arising from the oxygen vacancies. The small canted angle between the moments of the Mn sublattices leads to a small ferromagnetic moment.[20]

$MnO_{2-\delta}$ microspheres have been synthesized using hydrothermal and room temperature chemical reaction methods. The microspheres consists of $MnO_{2-\delta}$ nanowires having a diameter of 20–50 nm and a length of 2–8 μm. The estimated value of the oxygen vacancy δ from XPS data is 0.3. The magnetic measurements indicate that MnO_2 has an antiferromagnetic structure with a parasitic ferromagnetic component below the Néel temperature, T_N. T_N is about 13 K, which is 10 K lower than that of bulk MnO_2 single crystals.

[1]X. F. Daun, Y. Huang, Y. Cui, J. F. Wang, and C. M. Lieber, Nature (London) **409**, 66 (2001).
[2]J. Hu, M. Ouyang, P. Yang, and C. M. Lieber, Nature (London) **399**, 48 (1999).
[3]J. R. Heath, P. J. Kuekes, G. Snyder, and R. S. Williams, Science **280**, 717 (1998).
[4]M. Huang, S. Mao, H. Feick, H. Yan, Y. Wu, H. Kind, E. Weber, R. Russo, and P. Yang, Science **292**, 1897 (2001).
[5]A. R. Armstrong and P. G. Bruce, Nature (London) **381**, 499 (1996).
[6]B. Ammundsen and J. Paulsen, J. Adv. Mater. **13**, 943 (2001).
[7]L. I. Hill, A. Verbaere, and D. Guyomard, J. Power Sources **119**, 226 (2003).
[8]Q. Li, J. B. Olson, and R. M. Penner, Chem. Mater. (in press).
[9]S. Bach, J. P. Pereira-Ramos, and N. Baffier, J. Solid State Chem. **120**, 70 (1995).
[10]J. C. Hunter, J. Solid State Chem. **39**, 142 (1981).
[11]M. H. Rossouw, D. C. Liles, and M. M. Thackeray, Mater. Res. Bull. **27**, 221 (1997).
[12]C. Wu, Y. Xie, D. Wang, J. Yang, and T. Li, J. Phys. Chem. B **107**, 13583 (2003).
[13]X. Wang and Y. D. Li, J. Am. Chem. Soc. **124**, 2880 (2002); Chem. Commun. (Cambridge) **2002**, 764.
[14]M. Zhuang and J. W. Halley, Phys. Rev. B **64**, 024413 (2001).
[15]H. Kawamura, J. Appl. Phys. **63**, 3086 (1988).
[16]H. Sato, K. Wakiya, T. Enoki, T. Kiyama, Y. Wakabayashi, H. Nakao, and Y. Murakami, J. Phys. Soc. Jpn. **70**, 37 (2001).
[17]N. Yamamoto, T. Endo, M. Shimada, and T. Takada, Jpn. J. Appl. Phys. **13**, 723 (1974).
[18]*Handbook of X-ray Photoelectron Spectroscopy*, edited by J. Chastain (Perkin-Elmer Corporation, Physical Electronic Division, USA), 79 pp.
[19]Kh. Ya. Mulyukov, R. Z. Valiev, G. F. Korznikova, V. V. Stolyarov, Phys. Status Solidi A **112**, 137 (1989).
[20]V. E. Naish and E. A. Turov, Fiz. Met. Metalloved. **11**, 321 (1961); **9**, 10 (1960).